LETTERS

The ITQ-37 mesoporous chiral zeolite

Junliang Sun[1], Charlotte Bonneau[1], Ángel Cantín[2], Avelino Corma[2], María J. Díaz-Cabañas[2], Manuel Moliner[2], Daliang Zhang[1], Mingrun Li[1] & Xiaodong Zou[1]

The synthesis of crystalline molecular sieves with pore dimensions that fill the gap between microporous and mesoporous materials is a matter of fundamental and industrial interest[1–3]. The preparation of zeolitic materials with extralarge pores and chiral frameworks would permit many new applications. Two important steps in this direction include the synthesis[4] of ITQ-33, a stable zeolite with 18 × 10 × 10 ring windows, and the synthesis[5] of SU-32, which has an intrinsically chiral zeolite structure and where each crystal exhibits only one handedness. Here we present a germanosilicate zeolite (ITQ-37) with extralarge 30-ring windows. Its structure was determined by combining selected area electron diffraction (SAED) and powder X-ray diffraction (PXRD) in a charge-flipping algorithm[6]. The framework follows the $SrSi_2$ (srs) minimal net[7] and forms two unique cavities, each of which is connected to three other cavities to form a gyroidal channel system. These cavities comprise the enantiomorphous srs net of the framework. ITQ-37 is the first chiral zeolite with one single gyroidal channel. It has the lowest framework density (10.3 T atoms per 1,000 Å^3) of all existing 4-coordinated crystalline oxide frameworks, and the pore volume of the corresponding silica polymorph would be 0.38 cm^3 g^{-1}.

Three-dimensional extra-large pore systems have been the realm of amorphous silica materials with wall structures corresponding to the primitive, diamondoid and gyroidal (G) periodic surfaces, with a significantly higher occurrence of the G-surface; only the latter exhibits chiral channels of opposite handedness on either side of the surface. The greater stability of the G-surface has been demonstrated mathematically[8] and is understood in the chemistry of mesoporous silica materials to be a favourable configuration for reducing the hydrophobic/hydrophylic interface during crystallization. With inorganic crystalline compounds, the ANA[9] framework remained the only zeolite following the G-surface until the discovery of UCSB-7[10] with 12-ring channels. The first crystalline oxide with pores larger than 20 Å was the germanate SU-M[11], with Ge in tetrahedral and octahedral coordination, which cannot be considered a zeolite. Its framework can be described as a reticulation of the G-surface. If we could direct the inorganic framework on one side of the G-surface, while leaving the other side empty, a zeolitic material with extralarge pores and channels displaying only one enantiomorph might be obtained. ITQ-37 is the first such zeolite.

The systematic exploration of the phase diagrams of germanosilicates by high-throughput techniques using three large dicationic organic structure directing agents (SDA1, SDA2 and SDA3; Supplementary Fig. 1) was the key for discovering the new zeolite ITQ-37 (see Methods). Whereas SDA1 and SDA3 gave beta-type materials or clathrasils, SDA2 produced ITQ-24[12] or a mixture of ITQ-24 and ITQ-37 (Supplementary Tables 1 and 2). SDA2 is a bulky diquaternary ammonium molecule (Fig. 1). We analysed the different synthesis parameters to find the synthesis conditions leading to pure ITQ-37 (see Methods and Supplementary Figs 2, 3 and 4). The chemical formula of ITQ-37 is $|(C_{22}N_2H_{40})_{10.5}(H_2O)_x|[Ge_{80}Si_{112}O_{400}H_{32}F_{20}]$, as obtained by combining the structure refinement and elemental analysis. SDA2 has been shown to be intact in the final product.

The germanosilicate ITQ-37 crystallizes in a cubic chiral space group ($P4_132$ or $P4_332$, $a = 26.5126(3)$ Å), as determined by combining SAED and PXRD (see Methods Summary). The high degree of overlapping reflections (>94% exact overlapping with $d > 1.2$ Å; Fig. 2) and the peak broadening due to the small crystal sizes (70–200 nm, Supplementary Fig. 4a) posed great challenges for the structure determination. Several complex zeolite structures were recently determined by combining transmission electron microscopy and PXRD[13–15]. Crystal structure factor phases obtained from high-resolution transmission electron microscopy (HRTEM) images were used to facilitate the structure solution from PXRD, using the FOCUS program[16] (which uses crystal chemical information) or the Superflip program (based on a charge-flipping algorithm)[17].

However, these methods could not be applied to ITQ-37 because ITQ-37 is much more electron beam sensitive than other zeolites, permitting only the observation of the approximate pore structure from HRTEM images (Supplementary Fig. 5). We developed a new strategy of combining SAED and PXRD to solve the structure of ITQ-37, because SAED extends to a higher resolution than do HRTEM images (Supplementary Fig. 5). Intensities of nearly 80% of the total unique reflections to a 3.3 Å resolution were extracted from the SAED patterns along the [100], [110], [111] and [120] directions using the program ELD[18]; those were used for the pre-repartitioning of overlapping reflections in PXRD. Of the 16 overlapping reflection groups with $2\theta < 26°$, the intensities of reflections within ten groups were significantly improved by the pre-repartitioning step and are close to the structure factor intensities of the final structure. The charge-flipping algorithm was then applied for the structure determination. A hundred runs of charge-flipping iterations were tested using the Superflip program[17]. Random initial phases were used for each run, and electron density histogram matching was applied during the iterations for further repartitioning of the overlapping reflections[6]. The ten electron density maps with the best R-values (<26%) were

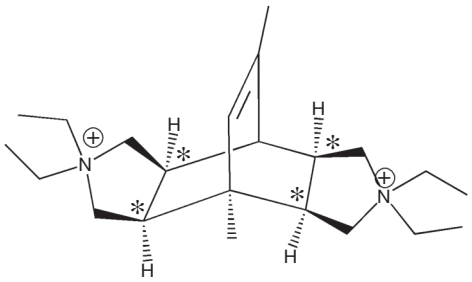

Figure 1 | Structure of SDA2 used for synthesizing the ITQ-37 zeolite. SDA2 contains four chiral centres (marked with asterisks) in a meso conformation, making the overall molecule achiral.

[1]Structural Chemistry and Berzelii Centre, EXSELENT on Porous Materials, Stockholm University, SE-106 91, Stockholm, Sweden. [2]Instituto de Tecnología Química (UPV-CSIC), Av. Naranjos s/n, E-46022 Valencia, Spain.

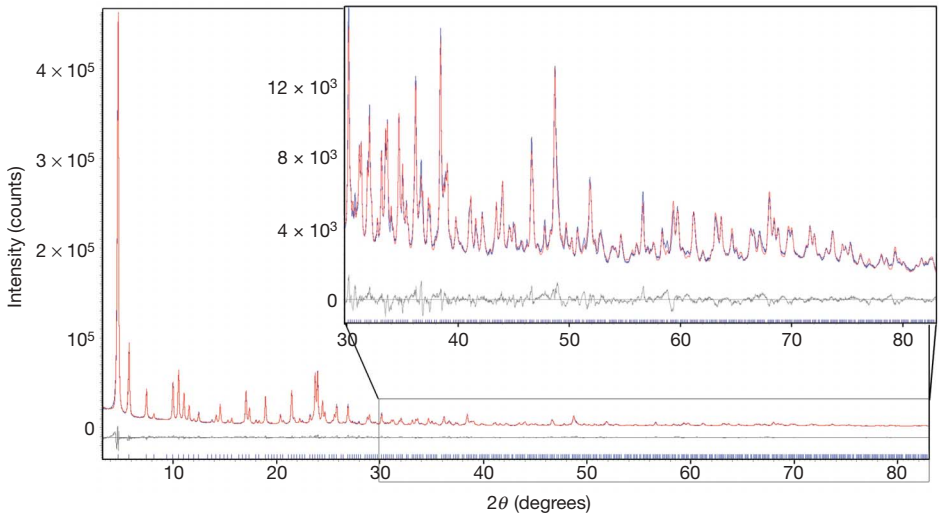

Figure 2 | Observed (blue), calculated (red) and difference (black) PXRD profiles for the Rietveld refinement of the as-synthesized ITQ-37 ($\lambda = 1.5406$ Å). The higher angle data ($2\theta = 30$–83°) has been scaled up (inset) to show the good fit between the observed and the calculated patterns.

examined and six of them showed similar pore features and framework structures.

Ten unique T atoms (in TO_4 tetrahedra, where T is an Si or Ge atom) and 18 of the 19 unique oxygen atoms could be automatically located from the best electron density map (lowest *R*-value, Fig. 3) by the EDMA program. One missing oxygen between T4 and T5 could easily be identified and thus added manually. The resulting structure is a three-dimensional framework, where Si and Ge atoms are tetrahedrally (T) coordinated with oxygen. All T–O and T–T distances are reasonable except for one ($d_{T4–T5} = 3.6$ Å). We note that the correct model could also be obtained without the pre-repartitioning but the convergence was slower and thus decreased the chance of success. The final framework structure was refined by Rietveld refinement with $R_p = 0.0381$, $R_{wp} = 0.0503$ and $R_{exp} = 0.0115$ (p, profile; wp, weighted profile; exp, expected) (Fig. 2, Methods Summary and Supplementary Table 3). All the bond distances and angles are reasonable in the refined structure. Eight of the ten unique T sites (T2 to T9) are shared by Si and Ge and the other two (T1 and T10) are occupied mainly by Ge, each coordinated to one hydroxyl group (Supplementary Table 4).

ITQ-37 has a very open framework consisting of one unique *lau* cage [$4^2 6^4$] and two unique double 4-rings [4^6]; both are recurring motifs in zeolites. Double 4-rings have one (D4R1) or two (D4R2) terminal hydroxyl groups (Fig. 4a). It is complicated to describe the framework of ITQ-37 using these units individually, so we chose a single tertiary building unit: $T_{44}O_{145}(OH)_7$ (where T = Si, Ge). The tertiary building unit has the point group C3 and is made up of one D4R1, three *lau* cages and three D4R2s (Fig. 4b). Each tertiary building unit is linked to three neighbouring building units, by sharing a common D4R2 and half of a 6-ring of the *lau* unit. There are eight such tertiary building units per unit cell, which lie on the nodes of a three-coordinated srs net (Fig. 4b)[19]. The srs net is compatible with a gyroidal theme and usually occurs as an enantiomorphous pair separated by the G-surface. This is also the case in ITQ-37. The gyroidal framework on one side of the G-surface generates a gyroidal channel system on the other side. The framework and the channel system have opposite handedness and both follow the srs net as an enantiomorphous pair (Fig. 4c). The channel system consists of two unique large cavities at the 4*a* and 4*b* positions (with coordinates 3/8, 3/8, 3/8 and 7/8, 7/8, 7/8 and their symmetry equivalents). Each large cavity communicates with three others through windows of thirty TO_4 tetrahedra (30-rings) with an asymmetric opening of 4.3 × 19.3 Å (Fig. 4c and Supplementary Fig. 6a), assuming the van der Waals diameter for oxygen of 2.7 Å. The D4R1s, D4R2s and *lau* cages individually follow the srs, srs-e (lcv) and srs-a nets, respectively[11,19]. All of these are chiral and of the same handedness as the

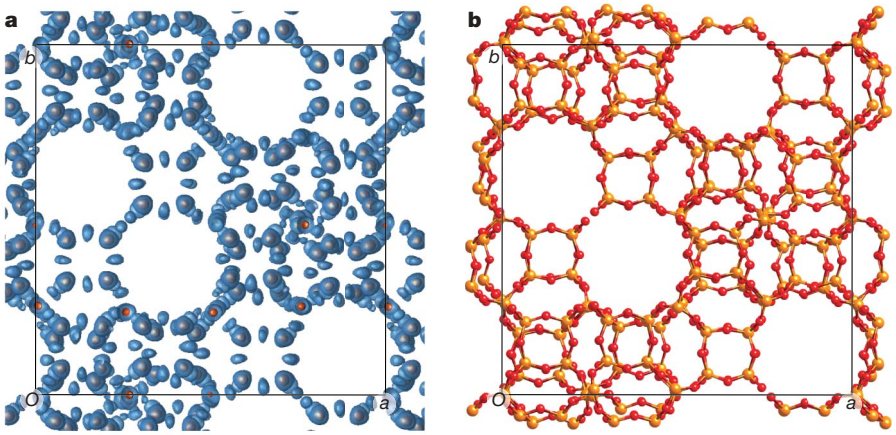

Figure 3 | Electron density map derived by the charge-flipping algorithm and the obtained structure model, both are viewed along the *c* axis. **a**, The electron density map is represented by two iso-surfaces at $2.7e$ Å^{-3} (in red) and $0.7e$ Å^{-3} (in blue), respectively (the maximum and minimum electron densities are $5.5e$ Å^{-3} and $-0.7e$ Å^{-3}, respectively). All T (Si and Ge) atoms and 18 of the 19 O atoms could be directly located from the map. **b**, The framework structure model of ITQ-37 deduced from **a**. The T atoms are in yellow and oxygen atoms are in red.

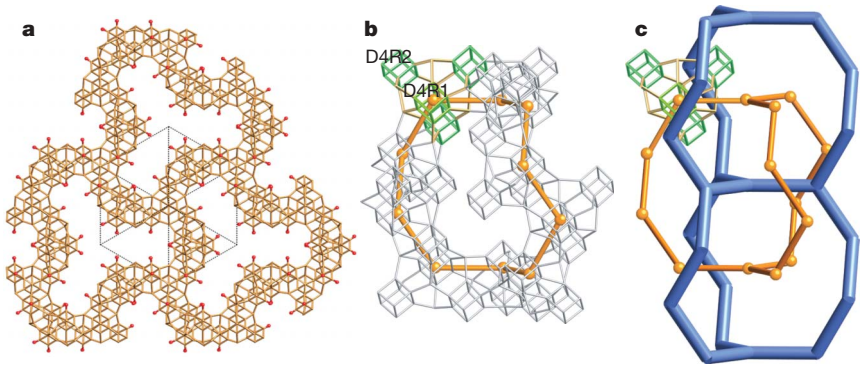

Figure 4 | The framework and corresponding nets of ITQ-37. a, A slice (15.3 Å thick) viewed down the [111] direction. Only the T–T connections and the terminal hydroxyl groups are shown. All double 4-rings have the same orientation. **b**, The 30-ring built from ten tertiary building units. One of them is highlighted (*lau* cage in orange and double 4-rings in green). The centres of the tertiary building units fall on the nodes of one srs net (in orange). **c**, The large cavity defined by three 30-rings. The centres of the large cavities fall on the nodes of another srs net (in blue) that represents the gyroidal channel system.

overall framework. The structure of the channel system (Supplementary Fig. 6b and c and Supplementary Movie 1) agrees with that observed in the HRTEM images (Supplementary Fig. 5c and d).

The ^{19}F magic-angle spinning nuclear magnetic resonance (MAS NMR) spectrum (Supplementary Fig. 7) shows a single resonance band at −10 p.p.m., characteristic for fluoride anions entrapped in germanium-rich double 4-rings. The ^{29}Si MAS NMR spectrum (Supplementary Fig. 8) shows two small peaks at −94 and −96 p.p.m., which correspond to structural defects in different crystallographic positions. The close proximity of protons to these Si sites is confirmed by the enhancement of these two peaks in the cross-polarization ^{1}H MAS NMR spectrum.

ITQ-37 is the first chiral zeolite with a single gyroidal channel. It has the lowest framework density of all existing 4-coordinated oxide frameworks, 10.3 T atoms per 1,000 Å^3. The tile representation (see Methods Summary) is a valuable tool for discerning the complex framework and channel system. The tertiary building unit is constructed of five different tiles: two corresponding to the double 4-rings, one to the *lau* cage (t-lau) and two interfacial tiles (6^3, t-kah) between the t-lau tiles (Fig. 5a and b). These tiles are commonly found in zeolites. The channel system is constructed of three tiles: two large tiles with similar volumes corresponding to the large cavities (Fig. 5c) and an interfacial tile (Supplementary Fig. 9). The tiling clearly demonstrates the opposite handedness of the channel system and the framework in ITQ-37 (Fig. 5c). It also offers a direct appreciation of the large accessible volume (Fig. 5d and Supplementary Movies 2 and 3). The BET (Brunauer–Emmett–Teller physical adsorption model) surface area of ITQ-37 is 690 $m^2 g^{-1}$, with a micropore volume of 0.29 $cm^3 g^{-1}$, as determined from the N_2 isotherm (Supplementary Fig. 10). We note that these values would correspond to a BET surface area of 900 $m^2 g^{-1}$ and a micropore volume of 0.38 $cm^3 g^{-1}$ for the silica polymorph of ITQ-37, which are far beyond the values previously reported for any zeolite structure.

The zeolite ITQ-37 shows a good thermal stability (Supplementary Fig. 11). A pelletized sample of ITQ-37 calcined at 813 K remained stable during two weeks while stored at room temperature in a moisture-free environment. Nevertheless, exposure to 90% humidity at room temperature led to a 20% and 50% loss of crystallinity after 10 h and 24 h, respectively. An Al-containing ITQ-37 sample ((Si+Ge)/Al = 70) was synthesized (Methods). The Al is tetrahedrally coordinated (Supplementary Fig. 12) and presents Brönsted acidity upon pyridine adsorption. Acetalyzation reactions require catalysts of mild acidities, and acetals are of interest for fine chemical industries[20–22], so we performed acetalyzation of aldehydes of different molecular sizes with triethyl orthoformiate using ITQ-37 as the catalyst to show the benefits of the large pores. We compared the catalytic results with those obtained on zeolite beta (Si/Al = 50) with a similar crystallite size (Supplementary Fig. 4 and Supplementary Table 5). For the smaller aldehyde (heptanal) that could diffuse in the pores of beta, both materials gave a similar initial activity. However for a larger aldehyde (diphenylacetaldehyde), the initial activity of ITQ-37 was almost three times that of beta. This indicates the presence of larger exploitable pores in ITQ-37 compared to those of beta. Furthermore, the selectivity to acetal at high conversion is much better for ITQ-37 with the bulkier aldehyde.

The discovery of the ITQ-37 zeolite has not only shown that zeolites can reach pore size dimension approaching the mesoporous range, but also provided new insight towards targeting chiral crystalline frameworks with extralarge pores. The success of this study arises from a combination of examining large non-surfactant molecules as

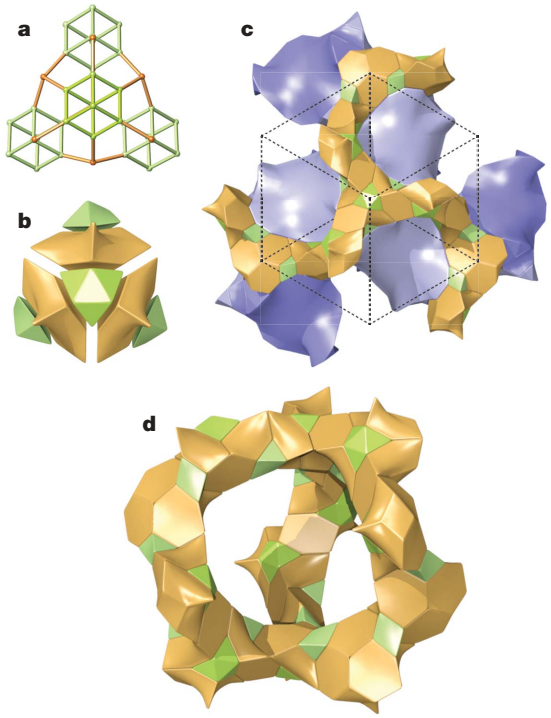

Figure 5 | Tiling of ITQ-37. a, The tertiary building unit $T_{44}O_{145}(OH)_7$ built from one D4R1, three D4R2s [4^6] and *lau* cages [$4^2 6^4$]. **b**, Tiles of the tertiary building unit in **a**. The interfacial tiles [6^3] are omitted for clarity and hydroxy-bearing T atoms were omitted for the tiling computation. **c**, Tiling of the framework (green and orange) and the channel system (blue), showing the large pore volume compared to the framework wall. The framework and channel systems have opposite chirality (left-handedness for the framework and right-handedness for the channel system). **d**, The srs large cavity defined by three 30-rings.

organic structure directing agents and the use of TEM and PXRD techniques in a new structure solution method.

METHODS SUMMARY

TEM characterization. TEM work was performed on JEM3010 electron microscopes under low-dose conditions (Supplementary Fig. 5). The 4- and 6-fold symmetries in SAED patterns indicated a cubic cell. The unit cell was determined from SAED patterns and further refined by PXRD to be $a = 26.5126(3)$ Å. The reflection condition $h00$: $h = 4n$ indicates that the space group is $P4_132$ or $P4_332$ (chiral with opposite handedness). The product is expected to be a racemic mixture owing to the achiral nature of the SDA2. The projection symmetries along the [100] and [111] directions are $p4gm$ and $p3m1$, respectively, determined from the phases extracted from Fourier transforms of HRTEM images using CRISP[23], which further confirmed the space group. The projected potential maps clearly show the pore structure that is consistent with the structure model (Supplementary Figs 5 and 6).

Structure determination. PXRD data were collected on a PANalytical X'Pert Pro. The structure was solved by charge-flipping algorithm combining SAED intensities and PXRD using the Superflip program[17]. The final structure model was refined by Rietveld refinement using TOPAS[24] with soft restraints for the T–O bond distances considering the Si/Ge occupancies. All T positions were refined with mixed occupancies of Si and Ge and a fixed overall Si/Ge ratio of 1.40, obtained from the elemental analysis. Although the organic structure directing agents were intact in the final product, as confirmed by the elemental analysis, they could not be located owing to their partial occupancies and lower symmetry. Instead, 12 unique carbon and four oxygen atoms were added at random positions inside the pores and refined subsequently. The PXRD pattern of the calcined sample also agrees with the structure model, but the diffraction peaks were too broad at the high angle region to perform a good refinement. This may be due to the collapse of the hydroxyl groups[15].

Topological analysis. The embedding of the tetrahedral net and tiling visualization were performed by Systre[25] and 3dt[26], respectively; both are part of the GAVROG project. The tiling data was computed with TOPOS[27].

Full Methods and any associated references are available in the online version of the paper at www.nature.com/nature.

Received 24 September 2008; accepted 6 March 2009.

1. Davis, M. E. Ordered porous materials for emerging applications. *Nature* **417,** 813–821 (2002).
2. Corma, A. State of the art and future challenges of zeolites as catalysis. *J. Catal.* **216,** 298–312 (2003).
3. Férey, G. Materials science: the simplicity of complexity—rational design of giant pores. *Science* **291,** 994–995 (2001).
4. Corma, A., Díaz-Cabañas, M. J., Jorda, J. L., Martínez, C. & Moliner, M. High-throughput synthesis and catalytic properties of a molecular sieve with 18- and 10-member rings. *Nature* **443,** 842–845 (2006).
5. Tang, L. Q. *et al.* A zeolite family with chiral and achiral structures built from the same building layer. *Nature Mater.* **7,** 381–385 (2008).
6. Baerlocher, Ch, McCusker, L. B. & Palatinus, L. Charge flipping combined with histogram matching to solve complex crystal structures from powder diffraction data. *Z. Kristallogr.* **222,** 47–53 (2007).
7. Delgado-Friedrichs, O., O'Keeffe, M. & Yaghi, O. M. Three-periodic nets and tilings: regular and quasiregular nets. *Acta Crystallogr. A* **59,** 22–27 (2003).
8. Schröder, G. E., Fogden, A. & Hyde, S. T. Bicontinuous geometries and molecular self-assembly: comparison of local curvature and global packing variation in genus-three cubic, tetragonal and rhombohedral surfaces. *Eur. Phys. J. B* **54,** 509–524 (2006).
9. Taylor, W. H. The structure of analcite ($NaAlSi_2O_6.H_2O$). *Z. Kristallogr.* **74,** 1–19 (1930).
10. Gier, T. E., Bu, X., Feng, P. & Stucky, G. D. Synthesis and organization of zeolite-like materials with three-dimensional helical pores. *Nature* **395,** 154–157 (1998).
11. Zou, X., Conradsson, T., Klingstedt, M., Dadachov, M. S. & O'Keeffe, M. A mesoporous germanium oxide with crystalline pore walls and its chiral derivative. *Nature* **437,** 716–719 (2005).
12. Cantín, Á., Corma, A., Díaz-Cabañas, M. J., Jorda, J. L. & Moliner, M. Rational design and HT techniques allow the synthesis of new IWR zeolite polymorphs. *J. Am. Chem. Soc.* **128,** 4216–4217 (2006).
13. Gramm, F. *et al.* Complex zeolite structure solved by combining powder diffraction and electron microscopy. *Nature* **444,** 79–81 (2006).
14. Baerlocher, Ch *et al.* Structure of the polycrystalline zeolite catalyst IM-5 solved by enhanced charge flipping. *Science* **315,** 1113–1116 (2007).
15. Baerlocher, Ch *et al.* Ordered silicon vacancies in the framework structure of the zeolite catalyst SSZ-74. *Nature Mater.* **7,** 631–635 (2008).
16. Grosse-Kunstleve, R. W., McCusker, L. B. & Baerlocher, Ch Powder diffraction data and crystal chemical information combined in an automated structure determination procedure for zeolites. *J. Appl. Cryst.* **30,** 985–995 (1997).
17. Palatinus, L. & Chapuis, G. Superflip—a computer program for the solution of crystal structures by charge flipping in arbitrary dimensions. *J. Appl. Cryst.* **40,** 786–790 (2007).
18. Zou, X. D., Sukharev, Y. & Hovmöller, S. Quantitative measurement of intensities from electron diffraction patterns for structure determination—new features in the program system ELD. *Ultramicroscopy* **52,** 436–444 (1993).
19. O'Keeffe, M., Peskov, M. A., Ramsden, S. J. & Yaghi, O. M. The Reticular Chemistry Structure Resource (RCSR) database of, and symbols for, crystal nets. *Acc. Chem. Res.* **41,** 1782–1798 (2008).
20. Climent, M. J., Corma, A. & Velty, A. Zeolites for the production of fine chemicals. Synthesis of the fructone fragance. *J. Catal.* **196,** 345–351 (2000).
21. Climent, M. J., Corma, A. & Velty, A. Design of a solid catalyst for the synthesis of a molecule with a orange blossom scent. *Green Chem.* **4,** 565–569 (2002).
22. Climent, M. J., Corma, A. & Velty, A. Synthesis of hyacinth, vanilla and orange blossom fragrances. The benefit of using zeikutes and delaminated zeolites as catalysts. *Appl. Catal. Gen.* **263,** 155–161 (2004).
23. Hovmöller, S. CRISP: Crystallographic image processing on a personal computer. *Ultramicroscopy* **41,** 121–135 (1992).
24. Young, R. A. *The Rietveld Method* 1–39 (IUCr Book Serials, Oxford Univ. Press, 1993).
25. Delgado-Friedrichs, O. & O'Keeffe, M. Identification and symmetry computation for crystal nets. *Acta Crystallogr. A* **59,** 351–360 (2003).
26. Delgado-Friedrichs, O. Data structures and algorithms for tilings. I. *Theor. Comput. Sci.* **303,** 431–445 (2003).
27. Blatov, V. A. Multipurpose crystallochemical analysis with the program package TOPOS. *IUCr Comp. Commun. Newsl.* **7,** 4–38 (2006).

Supplementary Information is linked to the online version of the paper at www.nature.com/nature.

Acknowledgements This project is supported by the CICYT (Project MAT 2006-14274-C02-01 and Prometeo 2008 GV), the Swedish Research Council (VR) and the Swedish Governmental Agency for Innovation Systems (VINNOVA). J.S. and C.B. are supported by post-doctoral grants from the Carl-Trygger and Wenner-Gren foundations respectively. M.M. thanks ITQ for a scholarship.

Author Contributions D.Z. and M.L. carried out the TEM work. J.S. solved and refined the structures. C.B. did the topological analysis. M.M., M.J.D.-C. and A.C. carried out the zeolite synthesis work. Á.C. synthesized the organic structure directing agents. J.S., C.B., A.C. and X.Z. wrote and corrected the manuscript.

Author Information Reprints and permissions information is available at www.nature.com/reprints. Correspondence and requests for materials should be addressed to A.C. (acorma@itq.upv.es) or X.Z. (zou@struc.su.se).

METHODS

Synthesis of SDA1 and SDA2. The starting materials for the synthesis of SDA1 and SDA2, were bicyclo[2.2.1]oct-7ene-2,3,5,6-tetracarboxylic dianhydride, and 4,6-dimethyl-α-pyrone and maleic anhydride, respectively.

To synthesise the Diels–Alder adduct from 4,6-dimethyl-α-pyrone and maleic anhydride, a toluene solution (500 ml) of 4,6-dimethyl-α-pyrone (161 mmol) and maleic anhydride (322 mmol) was refluxed for 5 days. After cooling, the resulting precipitate was filtered and washed with hexane to give the corresponding bicyclodianhydride (87%).

To aminate the bicyclodianhydrides, we dissolved the bicyclodianhydride products (140 mmol) in ethylamine solution (70% in H_2O) (400 ml) and refluxed for 3.5 days. After cooling, the solvent was removed in vacuum, providing the desired diimides in quantitative yields.

To reduce the diimides, we slowly added the corresponding diimide (49 mmol) to a suspension of $LiAlH_4$ (244 mmol) in anhydrous THF (300 ml) under N_2 and at 0 °C. When the addition was finished the mixture was refluxed for 5 h and stirred at room temperature overnight. The reaction was then quenched by addition of H_2O (10 ml), 15% aqueous solution of NaOH (10 ml) and distilled H_2O (10 ml). After 30 min stirring at room temperature the solution was filtered, partially concentrated under vacuum and then extracted with dichloromethane. The combined organic extracts were washed with brine, dried and concentrated to dryness to yield the corresponding amines (66%).

To alkylate the diamine, we added iodomethane (642 mmol) to a solution of diamine (52 mmol) in 70 ml of methanol. The mixture was stirred at room temperature for 72 h and methyl iodide (642 mmol) was added and stirred for an additional 72 h. The final organic dications were then concentrated under vacuum and precipitated by addition of diethyl ether. The precipitate was filtered under vacuum, yielding 20.8 g (89%) of the diquaternary ammonium as di-iodide salt.

Synthesis of SDA3. The starting materials for the synthesis of SDA3 were *N*-methylmaleimide and benzene.

For the cycloaddition of *N*-methylmaleimide and benzene, a solution of *N*-methylmaleimide (108 mmol) in a mixture of benzene (300 ml), acetophenone (30 ml) and acetone (84 ml) was distributed in ten Pyrex tubes. Before the photochemical reaction, N_2 was flowed through the solutions for 15 min and then the solutions were irradiated with a high-pressure mercury lamp ($200\ nm < \lambda < 90\ nm$) while stirring for 48 h. The resulting precipitate was filtered under vacuum to yield the desired diimide (40%).

To reduce the diimide, we slowly added the corresponding diimide (49 mmol) to a suspension of $LiAlH_4$ (244 mmol) in anhydrous THF (300 ml) under N_2 and at 0 °C. The mixture was then refluxed for 5 h and stirred at room temperature overnight. The reaction was quenched by addition of H_2O (10 ml), 15% aqueous solution of NaOH (10 ml) and distilled H_2O (10 ml). After 30 min stirring at room temperature (about 25 °C) the solution was filtered, partially concentrated under vacuum and extracted with dichloromethane. The combined organic extracts were washed with brine, dried and concentrated to dryness to yield the corresponding diamine (70%).

To alkylate the diamine, we added a solution of the diamine (33.5 mmol) in methanol (85 ml) to CH_3I (1.7 mol). The mixture was stirred for 7 days at room temperature. The mixture was concentrated under vacuum to yield the desired diammonium salt (75%).

Synthesis of ITQ-37. Synthesis gels were prepared using an automated system, composed of a robotic arm for vial handling and weighing of solids, a stirring station for gel homogenization and evaporation, a liquid dosing station equipped with pumps and an analytical balance.

The typical automated synthesis procedure is as follows: GeO_2 and boric acid (99.5%, Aldrich) or alumina (74.6%, Condea) were dissolved in the structure directing agent hydroxide solution. Then colloidal silica (Ludox AS-40, Aldrich) was added, and finally, a solution of NH_4F (98%, Aldrich).

The synthesis gel was transferred to Teflon vials (3 ml), which were finally inserted in a 15-well multiautoclave. Crystallization was carried out at 175 °C under static conditions. After filtration, washing and drying, the samples were characterized by PXRD using a multi-sample Phillips X'Pert diffractometer employing Cu Kα radiation.

The compositions of two typical synthesis gels to obtain ITQ-37 are as follows: $0.5\ SiO_2{:}0.5\ GeO_2{:}0.25\ SDA2(OH)_2{:}0.50\ NH_4F{:}3\ H_2O$, without aluminium, and $0.5\ SiO_2{:}0.5\ GeO_2{:}0.01\ Al_2O_3{:}0.25\ SDA2(OH)_2{:}0.50\ NH_4F{:}3\ H_2O$, with aluminium. Crystallization was carried out at 175 °C over 24 h under static conditions.

Catalytic experiments. Activation of 100 mg of the catalyst was performed *in situ* by heating the solid at 110 °C under vacuum for 3 h. After this time, the system was left to cool down to room temperature and then a solution of the carbonyl compound (Aldrich) (3 mmol) and triethyl orthoformate (98%, Aldrich) (11 mmol) in tetrachloromethane (Panreac, 25 ml as solvent) was poured onto the activated catalyst. The resulting suspension was magnetically stirred at reflux temperature. Aliquots were analysed at different reaction times by means of gas chromatography (HP-5 column), while products were identified by mass spectroscopy. The response factors of the different compounds were determined to calculate accurately the conversion and selectivity of the process.